

1 Performance of low noise fans in power plant air cooled steam condensers

2 Sybrand J. van der Spuy^{a)}, Theodor W. von Backström^{b)} and Detlev G. Kröger^{c)}

3 (Received: 09 January 2008; Revised: 13 May 2008; Accepted: 18 May 2008)

4 **Axial fans are often installed in locations where the orientation and surrounding**
5 **infrastructure can have a detrimental effect on the fan performance indicated**
6 **by the manufacturer. This paper addresses various aspects of phenomena**
7 **related to the installation of axial fans, one of these being the use of low-noise**
8 **fans, and how these can be considered in the CFD performance evaluation of**
9 **modern air-cooled power plant condensers. © 2009 Institute of Noise Control**
10 **Engineering.**

11 Primary subject classification: 11.4.1; Secondary subject classification: 53.1

12

13 1 INTRODUCTION

14 In air-cooled power plant steam condensers, cooling
15 is achieved by blowing air across the finned tube
16 bundles arranged in the form of an A-frame above
17 large-diameter axial flow fans (see Fig. 1). The fans are
18 installed with the plane of rotation horizontally and are
19 driven by electric motors through a gearbox. The fan
20 and A-frame units are arranged in series to form a fan
21 row, with a number of fan rows serving a single turbine
22 unit in parallel. The result is that a power station will
23 have a large array of fan units depending on the number
24 of turbine units. The world's largest direct air-cooled
25 power plant has an array of 288 axial fans, 9.1 m in
26 diameter, located 45 m above ground level¹.

27 The performance characteristics of these fans have
28 to be such that a prescribed air flow rate is guaranteed
29 for specified flow resistances caused by the heat
30 exchanger bundles and other obstructions, and by
31 non-ideal flow patterns, while at the same time not
32 exceeding prescribed noise levels. The required flow
33 rate, coupled to the pressure losses, is regarded as the
34 primary performance requirements of an installation,
35 since it is directly linked to the effectiveness of the
36 power generation process. The prescribed noise level is
37 seen as a secondary requirement that is based on
38 regulatory restrictions, often linked to the location of
39 the installation. If a fan does not meet the primary
40 performance requirement, it often exhibits increased

noise levels due to increased unsteadiness in the flow².
Neise² referred to tests done with a 90° duct bend at
various axial distances upstream of an axial flow fan.
He reported that at short distances, the low frequency
random noise components were increased by as much
as 14 dB, while at the blade passing frequency an
increase in the order of 7 dB was observed.

Recirculation of hot plume air and poor performance
of the fans located near the edges of the array have
been observed in large air-cooled steam condensers. In
extreme cases, backflow of air through the fan occurred
during windy periods^{3,4}. The orientation of the fans
means that their axes of rotation are vertical. The fans
therefore have flow entering from a direction that is
perpendicular to its axis of rotation. This causes fan
inlet losses due to the separation of flow at the lip of the
fan inlet as well as the off-axis inflow of air into the fan.
Fans that are located near the edge or periphery of the
array of air cooled condensers are severely affected by
flow separation, while off-axis inflow occurs
widespread through all fans installed in the array⁵.

a) University of Stellenbosch, Department of Mechanical Engineering, Private Bag X1, Matieland, 7602, SOUTH AFRICA; email: sjvdspuy@sun.ac.za

b) University of Stellenbosch, Department of Mechanical Engineering, Private Bag X1, Matieland, 7602, SOUTH AFRICA; email: twvb@sun.ac.za

c) University of Stellenbosch, Department of Mechanical Engineering, Private Bag X1, Matieland, 7602, SOUTH AFRICA; email: dgk@sun.ac.za

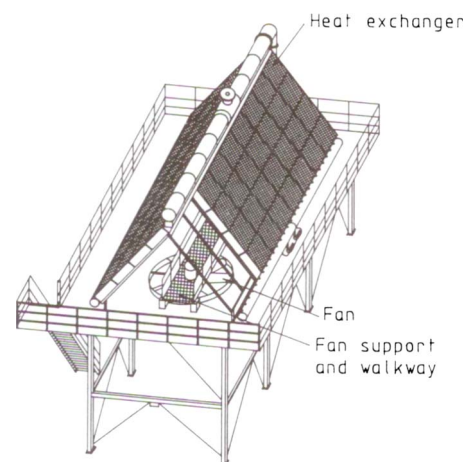


Fig. 1—Typical A-frame air-cooled condenser (Kröger¹).

62 Stinnes et al.⁶ derived a relatively simple, though
 63 highly effective, model to describe the decrease in
 64 performance due to off-axis inflow, based on a series of
 65 experiments during which fans were tested with inlet
 66 ducts at specific angles to the fan plane of rotation. A
 67 number of authors have modelled and investigated the
 68 inlet loss effect on fan performance using computa-
 69 tional fluid dynamics (CFD)^{3-5,7,8}. The circumferential
 70 variation in inlet conditions directly upstream of the fan
 71 rotation plane causes a significant cyclic variation in
 72 the loading of the fan blades and consequently acts as a
 73 source of fan blade fatigue and fan noise^{2,9}. The use of
 74 CFD would potentially enable the plant designer or
 75 more specifically the fan designer, to make the neces-
 76 sary adjustments to the plant and fan design to
 77 minimize inlet losses. Unfortunately the use of CFD to
 78 model these conditions also has its limitations.

79 Due to the occurrence of backflow through some
 80 sections of the fan, conventional, simplified CFD fan
 81 models that only take into account the forward flow
 82 operation of a fan are not representative. Under these
 83 conditions the use of a full 3-dimensional CFD model
 84 of the fan or a novel “actuator disk model”¹⁰ is recom-
 85 mended. These models are both however computation-
 86 ally intensive and therefore a simpler approach,
 87 referred to as the “pressure jump model”, can be
 88 applied when flow distortions are less prominent. A
 89 number of fan installation and fan configuration effects
 90 have been investigated using this combination of
 91 methods. These will be discussed in more detail in this
 92 document.

93 2 THE ACTUATOR DISK MODEL

94 2.1 General Description

95 The actuator disk model and its application in CFD
 96 have been well researched and described in much detail
 97 by Meyer et al.¹⁰ The actuator disk model simulates the
 98 effect of the individual fan blades on the flow field
 99 using blade element theory (see Fig. 2).

100 The lift and drag forces, δ_L and δ_D , [N] acting on a
 101 fan blade element of radial length δr [m] are calculated
 102 using the following equations:

$$103 \quad \delta_L = \frac{1}{2} \rho |W_\infty|^2 C_L \times c \times \delta r \quad (1)$$

$$104 \quad \delta_D = \frac{1}{2} \rho |W_\infty|^2 C_D \times c \times \delta r \quad (2)$$

105 where ρ is the air density [kg/m³], W_∞ is the average
 106 relative velocity over the blade element [m/s], C_L and
 107 C_D are the coefficients of lift and drag (obtained from
 108 standard airfoil data based on an angle of attack α) and
 109 c is the average chord length of the blade element [m].

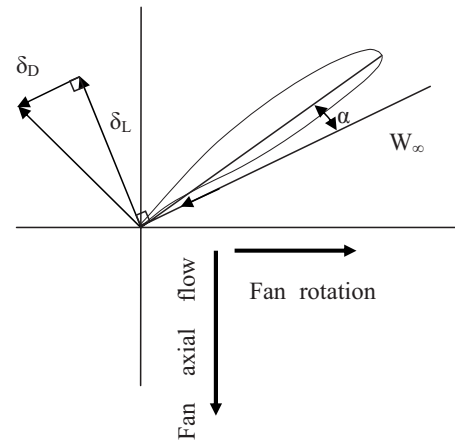


Fig. 2—Fan blade element.

Once the forces acting on the air stream are known,
 these are transformed into source terms that are
 inserted into the equation for linear momentum as
 follows:

$$s - \nabla p + \nabla \cdot \tau_{ij} = \rho \frac{dV}{dt} \quad (3)$$

where s is the per volume force vector of source terms
 [N/m³], ∇p is the gradient of static air pressure
 [N/m³], τ_{ij} is the shear stress tensor [N/m²] and V is
 the absolute velocity vector of the flow field [m/s].

2.2 Fan Model Validation

The fan considered in this analysis was a 9.145 m
 diameter, 8-bladed, cooling fan with a hub-to-tip ratio
 of 0.15, operating at 125 RPM (referred to as the
 A-fan). Details of the fan blade chord distribution,
 angle distribution and profile lift and drag coefficients
 are presented by Bredell¹¹. Bredell calculated the lift
 and drag coefficients for the blade profile over a range
 of -180° to $+180^\circ$ using CFD. This enabled the actua-
 tor disk model to solve the momentum source terms for
 flow coming from any direction (including backflow)
 through the rotor disk. The actuator disk model used in
 this analysis was validated by comparing results from
 the supplier fan curve to results obtained using the
 actuator disk model (see Fig. 3), where Y_{pt} refers to a
 setting angle at the blade tip based on the line tangent
 to the bottom of the blade profile. The results obtained
 from the actuator disk model were calculated according
 to the guidelines of the test standard used by the
 supplier, namely BS 848 part 1 (1980), type A¹². The
 results show excellent correlation between the supplier
 and simulated data in the operating range of the fan
 (between 500 m³/s and 700 m³/s) for the fan static
 pressure.

All CFD simulations were performed using
 FLUENTTM version 6.2.16. To model the test condi-

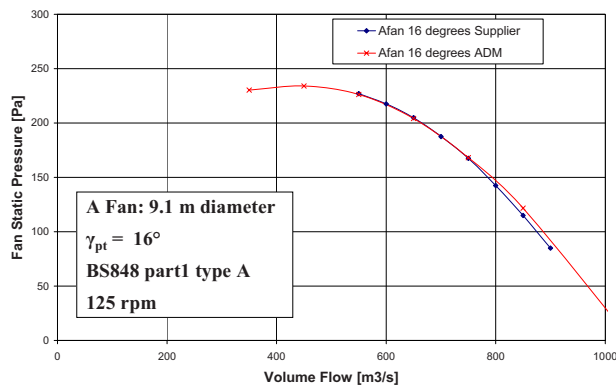


Fig. 3—Actuator disk model validation (fan static pressure).

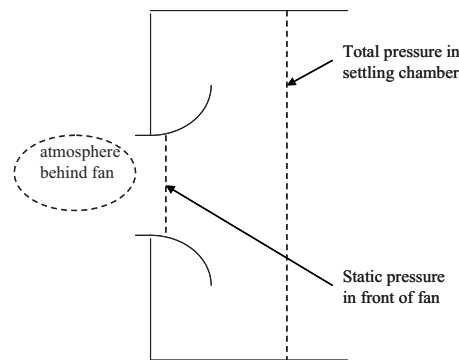


Fig. 4—Derivation of static-to-static pressure jump.

145 tions dictated by the British Standards, the inlet bound-
 146 ary was specified to be a mass flow inlet, while the
 147 outlet boundary was specified to be a total pressure
 148 boundary (pressure value set to atmospheric). To allow
 149 for dissipation of the fan exhaust dynamic component,
 150 the exhaust atmosphere was modelled to have a
 151 diameter of $4 \times$ fan diameter and a length of $8 \times$ fan
 152 diameter. The CFD model contained 550000 cell
 153 volumes. The validated CFD model used the realizable
 154 $k-\varepsilon$ model¹³ to simulate turbulence and the QUICK¹⁴
 155 interpolation scheme to calculate variables at the cell
 156 faces. The simulation was allowed to run for 3000 itera-
 157 tions or a residual value of 10^{-4} . Although the simula-
 158 tions were stable, convergence at flow rates less than
 159 $500 \text{ m}^3/\text{s}$ were not good.

160 3 THE PRESSURE JUMP METHOD

161 3.1 General Description

162 The motivation behind considering the use of a
 163 pressure jump method lies in its potential ability to
 164 model an array of axial fans accurately using a reduced
 165 number of cell volumes in CFD. The pressure jump
 166 method detailed in this document is in essence the
 167 same technique as that used by van Staden⁴ to model
 168 the performance of axial fans. The difference between
 169 the method detailed in this document (referred to as the
 170 “pressure jump method”) and the one used by van
 171 Staden is however the way in which the effect of the fan
 172 is implemented into the CFD code. The pressure jump
 173 method assumes a static-to-static pressure jump that
 174 occurs at the location of the fan rotation plane. This
 175 static-to-static pressure value is added to the static
 176 pressure term of the linear momentum equation in the
 177 flow field directly upstream of the fan rotation plane,
 178 shown in Eqn. (3).

179 Hotchkiss et al.⁵ and Stinnes et al.⁶ found that under
 180 cross-flow conditions (that lead to off-axis inflow) the
 181 “fan static pressure” is reduced in magnitude by the

dynamic pressure associated with the cross-flow 182
 component immediately upstream of the fan (“fan 183
 static pressure”, as referred to by typical fan supplier 184
 data and simulated by the actuator disk model is 185
 actually fan total-to-static pressure). The cross flow 186
 component affects the static pressure in front of the fan 187
 and not the actual value of static-to-static pressure 188
 increase. This is shown by Hotchkiss et al.⁵ to be attrib- 189
 uted to the fact that the cross flow effect on flow angles 190
 and velocities over the fan blades effectively cancels 191
 out when considering a fan rotor with blades running 192
 with and against the direction of cross flow. Based on 193
 these results the pressure jump method should yield 194
 accurate results when analysing fans subjected to cross 195
 flow only. The same can however not be said for flow 196
 separation that occurs over a localised area in front of 197
 the fan rotation plane. It is therefore expected that, 198
 although the pressure jump method would identify 199
 possible problematic intakes at the side of an axial fan 200
 array, the results would not be accurate and a more 201
 accurate analysis would be required. 202

The fan supplier data was compiled for a type-A fan 203
 installation (see Fig. 4). The fan pressure data is 204
 derived from an average static pressure value that is 205
 measured in a plane, relative to atmosphere, in a 206
 settling chamber, 1.25 fan diameters upstream from the 207
 fan, where the axial velocity is specified to be less than 208
 2 m/s . The static pressure measured in this location is 209
 assumed to equal the total pressure in this location. The 210
 total pressure loss between the measurement plane and 211
 the fan rotation plane is considered negligibly small 212
 because of the smooth bell mouth inlet (as specified by 213
 BS 848¹²). 214

To calculate the static pressure directly upstream of 215
 the fan rotation plane, as required for the pressure jump 216
 method, the dynamic pressure in the fan rotation plane 217
 is added to the “fan static pressure” curve. During the 218
 validation of the pressure jump method, it was found 219
 that the initial assumption of zero total pressure losses 220
 between the measurement plane and fan rotation plane 221

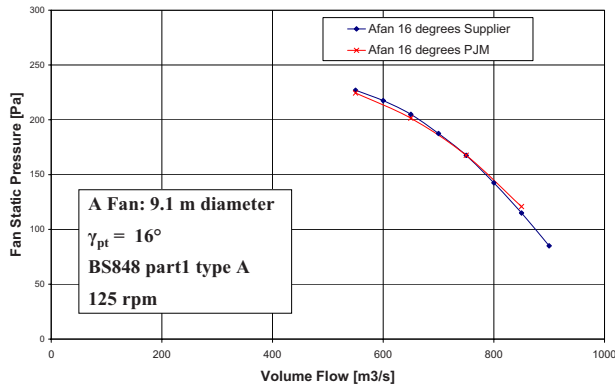


Fig. 5—Pressure jump method validation (fan static pressure).

was not sufficiently accurate and a loss coefficient was subsequently added. A value of 0.07 was used for the loss coefficient, which was based on flow data for rounded inlets, published by Idelchik¹⁵. The “fan static pressure” curve was therefore translated into a pressure jump value as follows:

$$\Delta p_{fan} = a + bV + cV^2 + dV^3 + \frac{1}{2}\rho V^2 + K_{loss}\frac{1}{2}\rho V^2 \quad (4)$$

where the values for a , b , c and d were derived from a curve-fit as described earlier, V is the average velocity perpendicular to the fan rotation plane [m/s] and K_{loss} is the described loss coefficient.

3.2 Fan Model Validation

The same geometric model that was used to validate the actuator disk method was used to validate the pressure jump method. Instead of using the described momentum sources, the standard FLUENT™ interface for specifying a pressure jump was used. The cell face region where the pressure jump would occur coincided with the fan rotation plane. The same boundary conditions, turbulence model and overall numerical differencing scheme were used as for the actuator disk method. The simulation was once again allowed to run for 3000 iterations or a residual value of 10^{-4} . The simulations were found to be stable and convergence generally occurred after 500 iterations. The resulting comparison of simulated and supplier data showed excellent correlation (see Fig. 5).

4 SIMULATION OF INSTALLED AXIAL FANS

4.1 Computational Model

To simulate the performance of axial fans under installed conditions, a 3-fan section of an array of air-cooled condensers was modelled (see Fig. 6).

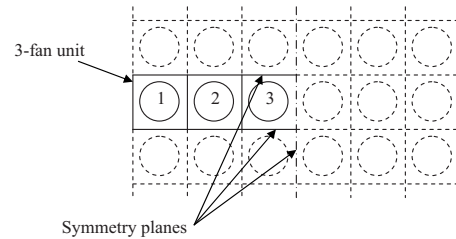


Fig. 6—A 3-fan section of an air-cooled condenser array, viewed from above.

Each of the fan units was modelled to consist of a bell mouth inlet, axial fan, rectangular plenum chamber and heat exchanger. The model had a total pressure boundary 200 m upstream from the fan array and a static pressure boundary 2 m downstream of the fan array (see Fig. 7). The analysis focussed on the inlet effects only, therefore the exit conditions of the system were simplified accordingly.

The heat exchanger was modelled as a porous region with resistance properties given by the equations from Bredell¹¹:

$$\Delta p_{HE} = - (4.132315 \times 10^{-4} Q^2 + 5.629484 \times 10^{-2} Q) \quad (5)$$

where Q is the volume flow rate through the heat exchanger [m³/s]. The above equation for system resistance coupled to the A-fan characteristics as shown in Fig. 3 corresponds to a reference flow condition of 650 m³/s.

4.2 Model Validation

The CFD model for a 14 m platform height contained 570000 cell volumes. The validated CFD model once again made use of the realizable k - ϵ model and the QUICK interpolation scheme. The CFD model for the 3-fan unit was validated by comparing the results from the model, using both the actuator disk model and pressure jump method to simulate the A-fan, with the empirical relation derived by Salta et al.¹⁶ The results showed the volumetric effectiveness of a multiple fan installation as a function of dimensionless platform height as follows:

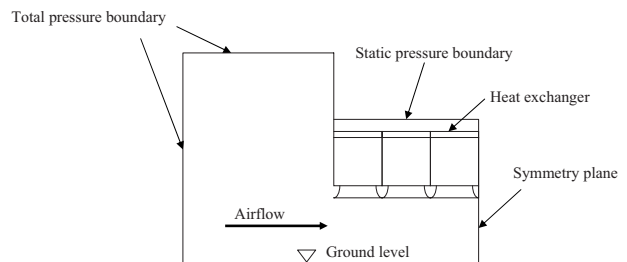


Fig. 7—Side view of computational domain for 3-fan unit.

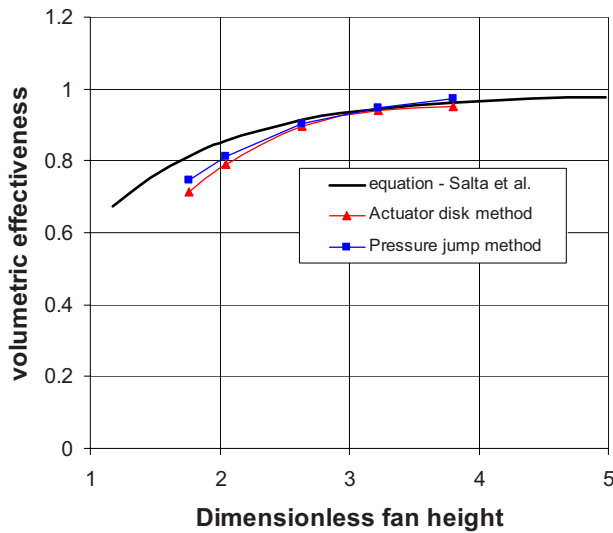


Fig. 8—Comparison of system volumetric effectiveness.

$$(Q/Q_{ref})_{system} = 0.985 - e^{-X} \quad (6)$$

where X is the dimensionless platform height:

$$X = \frac{(1 + 45/n) \times H}{6.35 \times D_F} \quad (7)$$

In the above equation, H is the platform height [m], n is the total number of fans per row (in other words 6 for the modelled 3-fan unit) and D_F is the fan shroud diameter [m]. The reference flow when determining the volumetric effectiveness (Q/Q_{ref}) of the installation was $650 \text{ m}^3/\text{s}$. A comparison of the results to the empirical correlation is shown in Fig. 8. The results show good correlation with the equation of Salta, at a dimensionless platform height between 2.5 and 4. The Salta fans had different ratios of dynamic pressure based on throughflow to pressure rise, compared to the A-fan. This leads to a different sensitivity to cross-flow and possibly to distortion and explains the difference in results at lower platform heights. Fig. 9 shows a vector plot with static pressure distribution to illustrate the extent of flow separation experienced by the edge fan of a multiple fan installation.

5 RESULTS

5.1 Fan Model Investigation

The 3-fan unit was first modelled by applying the actuator disk model in all three fans and subsequently compared to results obtained by applying the pressure jump method in all three fans. It was finally compared to a simulation using the actuator disk model on the “edge” fan only, combined with using the pressure jump method on the two inner fans. The actuator disk model is applied to the “edge” fan because of its ability

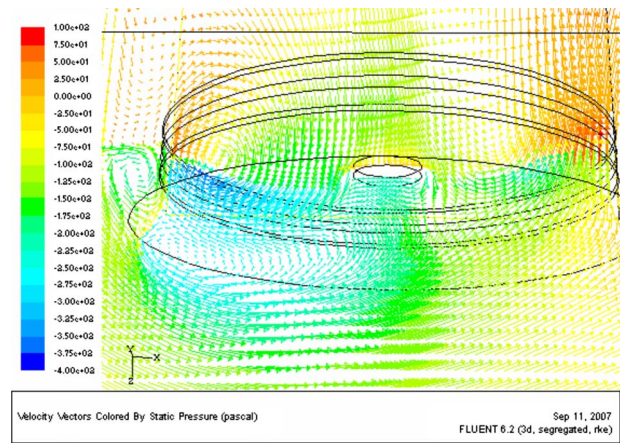


Fig. 9—Vector plot at fan inlet illustrating recirculation zone.

to simulate fan operation when backflow occurs through the fan. The results compare volumetric effectiveness at a height of 14 m and are shown in Fig. 10.

5.2 Platform Height Investigation

The 3-fan unit, using the above combination of fan models, was modelled with various platform heights, ranging from 14 m to 26 m as shown in Fig. 11.

5.3 Fan Geometry Investigation

The combined 3-fan unit was modelled with the standard 9.145 m cooling fan described in this document. This fan is referred to as the “A-fan” by Bredell et al.⁹ and has a hub-to-tip ratio of 0.15. The alternative fan was also a 9.145 m fan but with a hub-to-tip ratio of 0.4 and is referred to as the “B-fan” by Bredell. Under standard test conditions, Bredell points out that the B-fan exhibits a much steeper fan static pressure to volume flow rate curve than the A-fan. This is typically found when referring to the performance curves of “low-noise” fans and is the result of a relatively larger value for fan solidity (see Fig. 12). The investigation effectively compares the volumetric effectiveness of a standard industrial

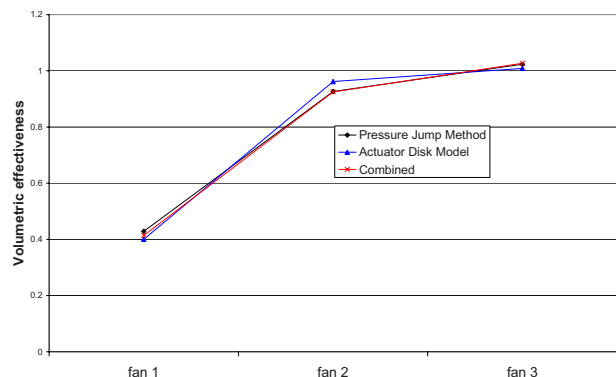


Fig. 10—Comparison of fan modelling methods.

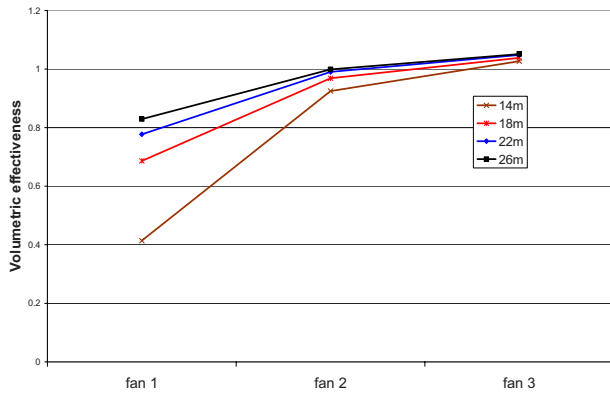


Fig. 11—Results from platform height investigation.

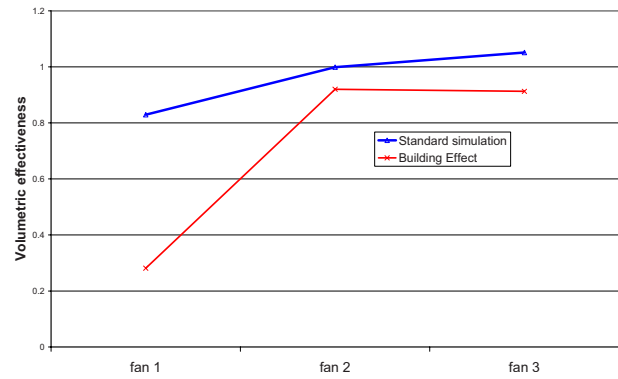


Fig. 14—The effect of buildings on the performance of a fan array at 26 m height.

336 cooling fan (A-fan) to a “low-noise” industrial cooling
 337 fan. The results for the 3-fan unit, comparing the
 338 volumetric effectiveness of the A-fan to that of the
 339 B-fan at a 14 m platform height is shown in Fig. 13.

340 5.4 System Configuration Investigation

341 To illustrate the possible application of the fan
 342 model, an investigation to show the effect of a building
 343 located a distance of 10 m upstream of the fan array on

the volumetric effectiveness of the fan array was 344
 conducted. The specific distance (10 m) was chosen 345
 purely as an example, although as a rule of thumb, any 346
 value in the order of or less than the specified platform 347
 height should have a detrimental effect on the volumet- 348
 ric effectiveness of the fans. It should be noted that the 349
 investigation only considered the effect on the inlet side 350
 of the fan array and no allowance was made for inter- 351
 action between the exhaust and inlet sides. The results 352
 for a platform height of 26 m are shown in Fig. 14. 353

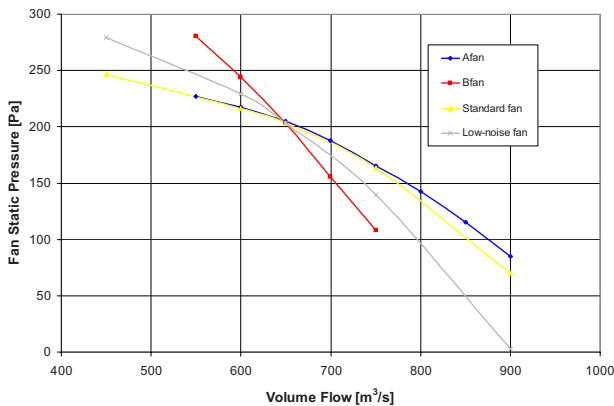


Fig. 12—Typical fan static pressure graphs for industrial fans.

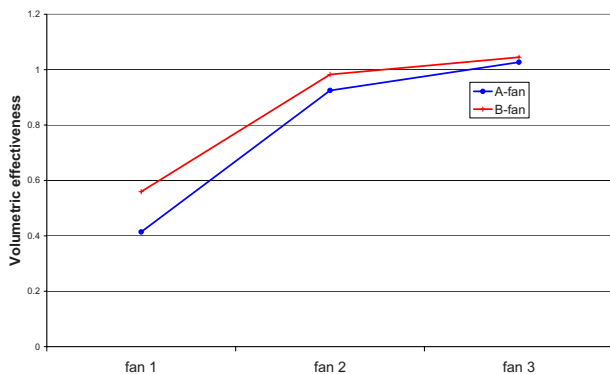


Fig. 13—Comparison of A-fan and B-fan performance at 14 m height.

6 DISCUSSION 354

This document describes various methods of 355
 simulating the performance of axial fans under 356
 installed conditions. The extent to which an air-cooled 357
 condenser plant can be modelled in CFD on a single 358
 processor is limited by the size of the geometry being 359
 modelled. Distorted inlet conditions generate flow 360
 separation at the edge of the fan inlet and off-axis 361
 inflow into the fans. The separation that occurs is 362
 localised on the edge-side of the inlet of the fans 363
 installed on the periphery of a fan array, while the 364
 off-axis inflow occurs on all fans installed in the fan 365
 array. The flow separation causes an off-balance inlet 366
 flow distribution that can be so severe that the edge fans 367
 experience back flow through the fan. The actuator disk 368
 model is therefore considered to be a good compromise 369
 when keeping the size of a CFD model to a minimum 370
 while still being able to model the effect that flow from 371
 various directions would have on the performance of a 372
 fan. Off-axis inflow is distributed across the whole face 373
 of a fan. Stinnes et al.⁵ has shown that for angles less 374
 than 45° the effects of off-axis inflow cancel out on 375
 opposing sides of the fan face. Off-axis inflow causes a 376
 pressure loss in front of the fan but does not alter the 377
 fan performance curve. The pressure jump method is 378
 therefore ideal in its application on fans operating in 379
 the first quadrant (positive pressure rise and positive 380
 volume flow) only. This limits its use to fans on the 381

382 inside of the fan array where flow separation is very
383 small to negligible.

384 It has been found that it is essential to validate the
385 fan models against results obtained under standard
386 BS848 test conditions to ensure that relevant turbu-
387 lence and discretization schemes are used. The actuator
388 disk model was found to be very stable when using a
389 first order discretization scheme for the continuity and
390 momentum equations but considerable effort (a more
391 detailed mesh and a larger outlet domain) was required
392 to improve this stability when using a second order
393 discretization scheme. It was also found essential to
394 validate the pressure jump method so that a loss coeffi-
395 cient could be specified that accounts for total pressure
396 losses between the measuring plane and the fan rotation
397 plane.

398 Considering application of these methods to the
399 modelling of power plant air-cooled steam condensers,
400 the following should be taken into account:

- 401 1. Non-uniform inlet flow, caused by flow separation
402 is a potential noise mechanism in a fan installa-
403 tion and any method that would dampen its
404 severity would therefore reduce the noise gener-
405 ated by the fan. Besides flow fluctuations, the
406 non-uniform inlet also causes local regions of
407 high relative velocities and a consequential large
408 increase in fan noise².
- 409 2. The volumetric effectiveness of a fan array de-
410 creases dramatically with platform height, pri-
411 marily due to the lower static pressure region be-
412 low the “edge” fans due to increased flow
413 separation in the fan inlet.
- 414 3. Fans having steeper fan static performance
415 curves, as typically exhibited by low-noise fans,
416 are less sensitive to flow distortions and exhibit a
417 higher volumetric effectiveness.
- 418 4. The volumetric effectiveness of a fan array de-
419 creases with the proximity of buildings since it
420 increases the cross flow velocity through the sys-
421 tem and causes more severe flow separation at
422 the edge fans.

423 Using the above CFD simulations, the user would be
424 able to quantify possible increases in plant operating ef-
425 ficiency and compare it to the additional cost required
426 for its manufacture. The biggest potential of the above
427 CFD simulations lie in their ability to model a fan array
428 accurately using a reduced number of cell volumes
429 (conservatively estimated, simplified CFD methods use

in the order of 10 times less cell volumes). This docu-
ment however only investigated and validated the prac-
tical application of these methods and further develop-
ment of the methods, specifically considering grid
dependency, is required.

7 REFERENCES

1. D. G. Kröger, *Air-cooled Heat Exchangers and Cooling Towers*, PennWell Corporation, Tulsa, OK, (2004).
2. W. Neise, “Installation effects on fan noise”, IMechE, C401/005, 83–91, (1990).
3. H. B. Goldschagg, F. Vogt, C. G. du Toit, G. D. Thiart and D. G. Kröger, “Air-cooled steam condenser performance in the presence of crosswinds”, *Proceedings: Cooling Tower Technology Conference, Electrical Power Research Institute*, Palo Alto, California, (1997).
4. M. P. van Staden, *An Integrated Approach to Transient Simulation of Large Air-cooled Condensers using Computation Fluid Dynamics*, D. Eng. Thesis, Department of Mechanical Engineering, Rand Afrikaans University, South Africa, (2000).
5. P. J. Hotchkiss, C. J. Meyer and T. W. von Backström, “Numerical Investigation into the effect of cross-flow on the performance of axial flow fans in forced draught air-cooled heat exchangers”, *Appl. Therm. Eng.*, **26**, 200–208, (2006).
6. W. H. Stinnes and T. W. von Backström, “Effect of cross-flow on the performance of air-cooled heat exchanger fans”, *Appl. Therm. Eng.*, **22**, 1403–1415, (2002).
7. G. D. Thiart and T. W. von Backström, “Numerical Simulation of the flow field near an axial fan operating under distorted inflow conditions”, *J. Wind. Eng. Ind. Aerodyn.*, **45**, 189–214, (1993).
8. J. R. Bredell, D. G. Kröger and G. D. Thiart, “Numerical Investigation of fan performance in a forced draft air-cooled steam condenser”, *Appl. Therm. Eng.*, **26**, 846–852, (2006).
9. J. R. Bredell, D. G. Kröger and G. D. Thiart, “Numerical Investigation into Aerodynamic Blade Loading in Large Axial Flow Fans Operating Under Distorted Inflow Conditions”, *R&D Journal*, **22**, 11–17, (2006).
10. C. J. Meyer and D. G. Kröger, “Numerical simulation of the flow field in the vicinity of an axial flow fan”, *Int. J. Numer. Methods Fluids*, **36**, 947–969, (2001).
11. J. R. Bredell, *Numerical investigation of fan performance in a forced draft air-cooled steam condenser*, M.Sc. Eng. Thesis, Department of Mechanical Engineering, University of Stellenbosch, South Africa, (2005).
12. *Fans for General Purposes, Part 1: Methods for Testing Performance*, British Standards 848 1980, British Standards Institution, London, United Kingdom, (1980).
13. T.-H. Shih, W. W. Liou, A. Shabbir, Z. Yang and J. Zhu, “A new k- ϵ eddy-viscosity model for high Reynolds number turbulent flows—model development and validation”, *Comput. Fluids*, **24**(3), 227–238, (1995).
14. B. P. Leonard, “A stable and accurate convective modelling procedure based on quadratic upstream interpolation”, *Comput. Methods Appl. Mech. Eng.*, **19**, 59–98, (1978).
15. I. E. Idelchik, *Handbook of Hydraulic Resistance*, 3rd Edition., Begell House, (1994).
16. C. A. Salta and D. G. Kröger, “Effect of inlet flow distortions on fan performance in forced draft air-cooled heat exchangers”, *Heat Recovery Syst. CHP*, **15**, 555–561, (1995).

AQ:
#1

NOT FOR PRINT!

FOR REVIEW BY AUTHOR

NOT FOR PRINT!

AUTHOR QUERIES — 001904NCE

#1 Au: Please provide coden/issn for Ref. 9